Integration of PEV and PV in Norway Using Multi-Period ACOPF — Case Study

Salman Zaferanlouei, Magnus Korpås, Hossien Farahmand, Vijay Venu Vadlamudi
Department of Electric Power Engineering
Norwegian University of Science and Technology
Trondheim, Norway

***Abstract*—Integration of Plug-in Electric Vehicles (PEVs) and renewables poses substantial challenges in electricity distribution networks. This paper investigates the impact of large-scale PEV penetration in distribution networks, when also considering the integration of other renewable energy resources, e.g., wind, hydropower and Photovoltaics (PVs). As such, analysis on an existing low voltage local power system is conducted through simulations. We propose an AC Optimal Power Flow (ACOPF) algorithm over a time horizon of several successive hours. The resulting optimisation framework considers the control of voltage fluctuations within safe bounds, and controlled charging of PEVs, taking into account the total energy consumption of users and the forecast generation of renewables. Simulation results show that the proposed algorithm saves the total cost when compared to an uncontrolled ('dumb') charging scenario.**

***Index Terms*—ACOPF, Multi-Period ACOPF, Plug-in Electric Vehicles, PV, Wind Power Plants, Optimal Charging.**

NOMENCLATURE

$\|Y_{ij}\|$	Magnitude of ij^{th} element in bus admittance matrix
Δt	Time step
$\eta_{chrg,i}, \eta_{dischrg,i}$	Charging and discharging efficiency of the PEV at i^{th} bus
$\lambda_{spot}(t)$	Electricity price in the wholesale market (spot price) at time t
θ_{ij}	Angle of ij^{th} element in bus admittance matrix
$E_{ST,i}(t)$	Energy stored in the PEV at i^{th} bus at time t
$E_{ST,i}^{max}$	Rated energy of the PEV at bus i
N	Total number of buses in the network.
$P_{DG,i}(t), Q_{DG,i}(t)$	Active and reactive power production from the distributed generator at i^{th} bus at time t
P_G	Active power flow from/to the upstream network.
$P_{LD,i}(t), Q_{LD,i}(t)$	Active and reactive power demand at i^{th} bus at time t
$P_{SCh,i}(t), P_{SDch,i}(t)$	Charging and discharging power of the PEV at i^{th} bus at time t
$P_{SCh,i}^{max}, P_{SDch,i}^{max}$	Rated charging and discharging capacity of the PEV at i^{th} bus
$Q_{DG,i}^{min}, Q_{DG,i}^{max}$	Minimum and maximum limit of the reactive power capability of the DG at i^{th} bus
$Q_{ST,i}(t)$	Reactive power supplied by the PEV at i^{th} bus at time t
S_{ij}	Apparent power flow from bus i to j
$SOC_i(t)$	State-of-charge of the PEV at i^{th} bus at time t
SOC_i^{min}, SOC_i^{max}	Minimum and maximum limit of the SOC at i^{th} bus
T	Total number of discrete intervals per planning horizon
$V_i(t), \delta_i(t)$	Voltage amplitude and the angle at i^{th} bus at time t
V_i^{min}, V_i^{max}	Minimum and maximum limit of the voltage amplitude at i^{th} bus

I. INTRODUCTION

In Norway, the introduction of incentive schemes for promoting electric vehicle users has accelerated the adoption of Plug-in Electric Vehicles (PEVs). All electric vehicles in Norway are exempt from taxation — value added tax and purchase tax. They are exempt from road tolls and parking fees in public parking spaces. Moreover, they have access to free battery charging at publicly funded charging stations, and are allowed to use collective transportation lanes [1]. As per 2017, Norway has the highest number of electric vehicles per capita in the world. PEVs are free of air pollutant emissions, and thus environmentally friendly, all the more so in Norway because 98% of the electricity production is from hydropower. Although PEVs help in the reduction of greenhouse gas emissions, high penetration of PEVs may result in significant technical issues in the distribution grids if charging is not properly coordinated. Uncoordinated charging of PEVs (also referred to as dumb charging) can overload the transformers, increase losses, cause under-voltage problems, and increase harmonic distortion [2], [3], [4]. Therefore, proper coordination of PEV charging with minimal negative effects on the distribution network is of utmost importance. Further, from an economic perspective, it is essential to have optimal scheduling of distributed generators in the distribution system, e.g., Photovoltaic (PV) systems and small-scale wind turbines, so that their energy production is maximally utilized.

Charging the PEVs during low electricity price period is economically attractive for the distribution system operator as well as the PEV owner. It is advantageous to shift the PEV load to periods when the grid is lightly loaded knowing that the electricity prices reflect the heavily loaded and lightly loaded times of the grid.

The Optimal Power Flow (OPF) solution is critical for the optimal operation of an electric power network over a specific time horizon, provided that both the load and the supply are deterministic. The application of AC Optimal Power Flow (ACOPF) for distribution systems is a recent development [5], [6], though several methods are in use and continue to be developed, for solving the general ACOPF problems efficiently [7], [8], [9], [10].

Optimisation of distribution networks with respect to wholesale market exchange including Distributed Energy Resources (DERs) has been explored in many papers. Some select-few literature survey highlights are as follows. Reference [11] pointed out the main aspects of DER, and the challenges and potential solutions in applying demand response in smart grids. Reference [12] proposed an algorithm for optimal coordination of DERs in active distribution networks. Reference [13] presented a mixed integer non-linear programming approach for determining optimal location and number of distributed generators in a hybrid electricity market.

In this paper, we present an optimal scheduling methodology for PEVs in a Norwegian distribution grid where significant amount of PVs and PEVs is accommodated. We use a multi-period ACOPF for finding the optimal charging schedule of the PEVs. Extensive simulations for different PEV-PV penetration scenarios are conducted to verify the flexibility introduced by PEVs and PVs, with respect to grid constraints. The rest of the paper is organised as follows. Section II explains the proposed multi-period ACOPF methodology. Section III presents the case study. Results from the simulations, and consequent discussion are provided in Section IV. Finally, conclusions are presented in Section V.

II. THE PROPOSED MULTI-PERIOD ACOPF METHODOLOGY

From the perspective of the distribution system operator, the charging of PEVs should be coordinated such that the cost of buying electricity from the upstream grid is minimised, while maintaining the quality of supply within the desired range, and ensuring that the loading on transformers and lines is well within their ratings. The overvoltage problem is a common problem that is experienced in residential areas with extensive distributed generators, especially PV[14]. The excess production from the PV system during the daytime when the network is usually lightly loaded causes reverse power flow. This can create overvoltage problems in some nodes in the network. On the other hand, PV generators do not produce power during nights. Usually peak load occurs in residential areas around 1800h - 2000h. During this period, network is prone to under-voltage problems. Charging the PEVs in this time slot can worsen the under-voltage problems. Therefore, due consideration must be given to the coordination of PEV charging. Moreover, it is advantageous if PEVs are charged using the production from the distributed generators within the system as much as possible. When there is not enough excess local production within the system, the required energy for PEV charging should be imported from the upstream grid. Hence, in order to minimise the cost of imported energy from the grid, batteries must be charged in time slots where electricity prices are the lowest.

A. Objective Function

The main objective of the distribution system operator is to minimise the cost of energy imported from the upstream grid over a certain time horizon.

$$Minimise \sum_{t=1}^{T} \lambda_{spot}(t).P_G(t) \tag{1}$$

B. AC Power Flow Equations

$$\begin{aligned} &P_{DG,i}(t) - P_{LD,i}(t) + P_{SDch,i}(t) - P_{SCh,i}(t) \\ &\quad = \sum_{j=1}^{N} |V_i(t)||V_j(t)||Y_{ij}|cos(\delta_j(t) - \delta_i(t) + \theta_{ij}) \end{aligned} \tag{2}$$

$$\begin{aligned} &Q_{DG,i}(t) - Q_{LD,i}(t) \\ &\quad = -\sum_{j=1}^{N} |V_i(t)||V_j(t)||Y_{ij}|sin(\delta_j(t) - \delta_i(t) + \theta_{ij}) \end{aligned} \tag{3}$$

C. Distributed Generator Constraints

$$Q_{DG,i}^{min} \leq Q_{DG,i}(t) \leq Q_{DG,i}^{max} \tag{4}$$

D. Voltage Constraints

$$V_i^{min} \leq V_i(t) \leq V_i^{max} \tag{5}$$

E. Line Constraints

The line constraints are apparent power flow limits in MVA:

$$|S_{ij}(\bar{\delta}, |\bar{V}|)| - S_{ij}^{max} \leq 0 \tag{6}$$

$$|S_{ji}(\bar{\delta}, |\bar{V}|)| - S_{ij}^{max} \leq 0 \tag{7}$$

F. PEV Constraints

$$\begin{aligned} 0 \leq P_{SCh,i}(t) \leq P_{SCh,i}^{max} \\ 0 \leq P_{SDch,i}(t) \leq P_{SDch,i}^{max} \end{aligned} \tag{8}$$

$$SOC_i^{min} \leq SOC_i(t) \leq SOC_i^{max} \tag{9}$$

$$SOC_i(t) = \frac{E_{ST,i}(t)}{E_{ST,i}^{max}} \tag{10}$$

$$\begin{aligned} &E_{ST,i}(t) = \\ &\quad E_{ST,i}(t-1) + \eta_{chrg,i} P_{Sch,i}(t)\Delta t - \frac{P_{SCch,i}(t)\Delta t}{\eta_{dischg,i}} \end{aligned} \tag{11}$$

The matrix solver also includes arrival and departure times of each PEV, which are not explicitly shown in the formulation above. Care has been taken in the implementation to ensure that the variables for charging and discharging do not conflict with each other. (A PEV can either be charging only or discharging only.)

III. Case Study

The proposed method is applied for scheduling the charging of PEVs in the Norwegian distribution grid, at location Steinkjer, in the district of Nord Trøndelag. The distribution grid consists of 32 distribution transformers (22 kV / 230 V), a small scale hydro power plant with rated capacity 2.4 MW, and 856 customers. The distribution grid is supplied by a 25 MVA, 66 kV / 22 kV transformer at the grid substation. Fig. 1 illustrates the single line layout of the 22 kV network of the grid. In this study, only the LV network supplied by the distribution transformer, indicated as DT1 in Fig. 1, is modelled in detail to consider the voltage variation on the LV side (230 V) of the network. The single line diagram of this LV network is shown in Fig. 2. The number of customers supplied by this network is 62. The highlighted houses in red in Fig. 2 indicate the critical voltage nodes of the network, which have been identified through AC power flow simulations. The other LV networks are modelled as aggregated loads connected to the secondary side of the transformers. The total number of buses in the resulting network is 147.

It is assumed that the distribution grid accommodates significant amount of distributed generators. The distributed generation includes rooftop PV generators and one aggregated wind farm generation. The selected location for the wind farm and its connection to the grid is shown in Fig. 1. The rated capacity of the proposed wind generator is 500 kW. The wind generator is connected to the 22 kV network using a 500 kVA, 690 V / 22 kV transformer. The power production from the wind generator was estimated using the wind measurement data provided by the utility company Nord-Trøndelag Elektrisitetsverk (NTE).

Different scenarios of PV installation were considered: 30%, 70%, 100% of the households have PV systems with rated capacity of 4 kW. The location of households with PV systems are randomly assigned. In the other part of the distribution grid, PV production is added as an aggregated production at the LV side of all the other 22 kV / 230 V transformers in the distribution network. The hourly power production from PV systems were estimated using the solar irradiance data at Steinkjer, the selected location. Load profiles of the consumers over a period of one year (2012) were obtained from NTE. The day with the highest demand (2 February) was chosen for the simulation. The average number of vehicles per household in Norway is 1.3 [15]. Accordingly, the number of PEVs in the LV network with 62 households supplied by the transformer DT1 is selected as 40 for a penetration level of 50%. Note that the aggregated charging of PEVs connected to the LV network supplied only by transformer DT1 is taken into account in this study.

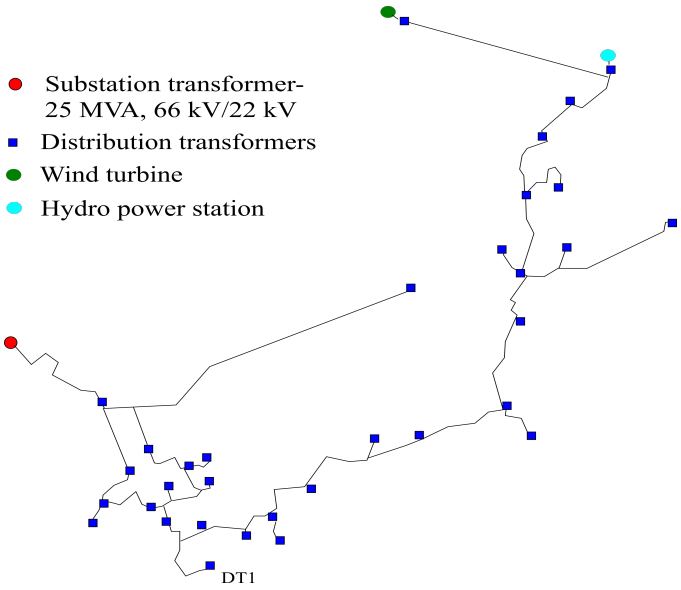

Fig. 1. Single-phase layout of the distribution network (22 kV).

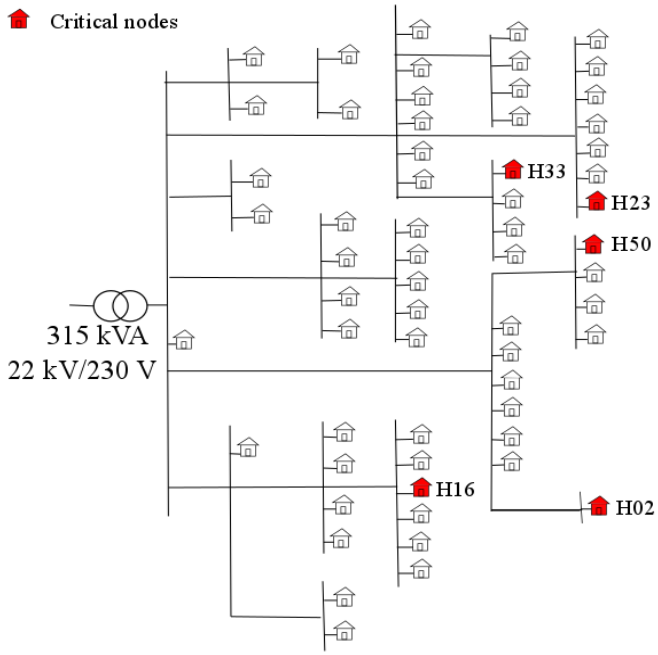

Fig. 2. LV network (230 V) supplied by the transformer- DT1.

The rated power and energy capacities of a single PEV are 6 kW and 20 kWh, respectively. Charging efficiency of all the PEVs is set at 85%. The maximum and minimum State-of-Charge (SOC) limits are set to 100% and 20%, respectively. Table I shows the arrival and departure times of PEVs in the residential area shown in Fig. 2 [15]. The arrivals begin at 1500 h and end at 2000 h. All departures take place the next day at 0800 h. For the case study, the optimisation problem was solved to obtain SOC, charging power and discharging power for each PEV at each hour.

TABLE I
ARIVAL AND DEPARTURE OF PEVS

Arrival		Departure	
Time(h)	Percentage (%)	Time(h)	Percentage(%)
1500	15	0800	100
1600	15	-	-
1700	40	-	-
1800	10	-	-
1900	10	-	-
2000	10	-	-

IV. RESULTS AND DISCUSSION

Fig. 3 illustrates the hourly power productions of hydropower, wind power plant and PVs for the configuration of the grid shown in Fig. 1. It also shows the hourly consumer load demand in the system on 2 Febuary, 2012. This a record peak demand for the year, and hence this worst-case scenario is chosen for the simulation.

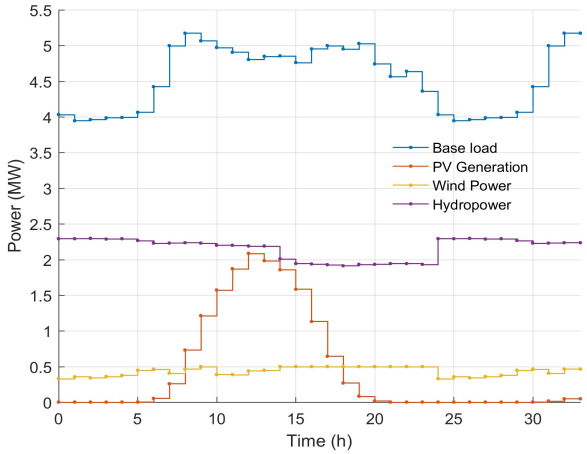

Fig. 3. Hourly average generation of wind, hydropower, aggregated PV and load data.

Fig. 4 shows the hourly power import into the distribution network; the corresponding electricity prices of the wholesale power market (Nord Pool) are also indicated. It can be clearly seen that the charging times are correlated with the lowest hourly electricity prices. However, charging power is only dependent on arrival time in the case of dumb-charging scenario.

Fig. 5 illustrates the charge behavior and SOC of individual PEVs located on the secondary side of transformer DT1. A comparison of the results of the proposed algorithm with those of the dumb-charging scenario are also shown in Fig. 5. From Fig. 5-a, it can be seen that charging occurs at the lowest marginal price around hours 25-31. However, for the dumb-charging scenario, the charging occurs at the arrival time. Fig. 5-b illustrates that the largest charge per hour can be 2.3 kW for the optimal charging scenario, whereas there is a constant profile for the dumb-charging scenario.

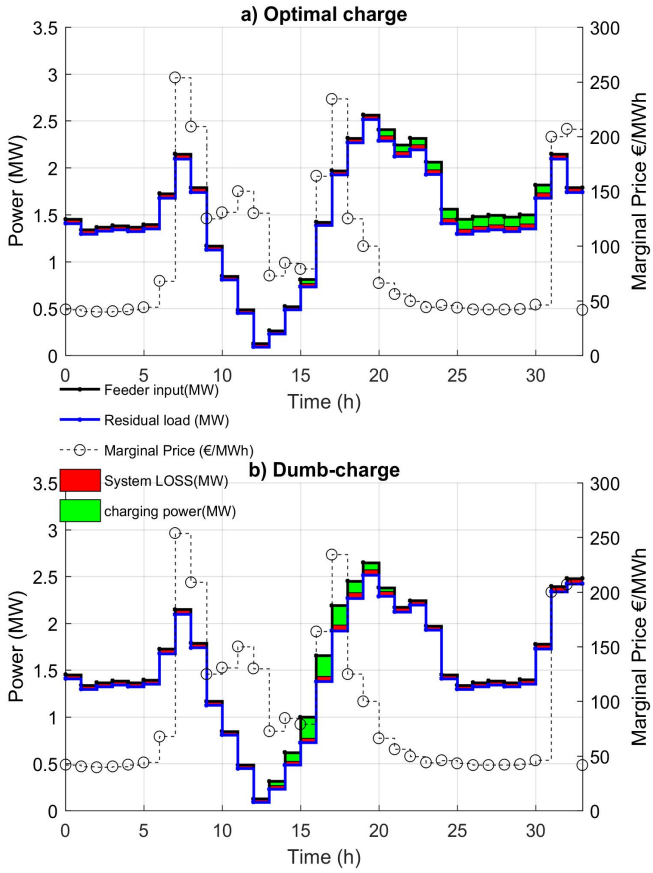

Fig. 4. 70% PEV and 100% PV penetration. Optimal charging profile with a) the proposed algorithm b) dumb-charging method.

Tables II and III present more detailed results of the simulations. Two ratio terms are defined: R_1 — ratio of the PV generation to the consumer energy demand in one cycle; R_2 — ratio of the PEV energy consumption to the consumer energy demand in one cycle. Note that consumer energy demand is the standard energy demand excluding the PEV energy demand. Table II shows the values of these ratios for different penetrations of PEV-PV in the distribution grid. These values show that PEV and PV have a smaller share compared to the actual consumer load demand in the distribution grid. One cycle is 24 hours from 0800 h of a day to 0800 h of the next day.

$$R_1 = \frac{PV \quad Generation \quad in \quad 1 \quad cycle}{Consumer \quad Energy \quad Demand \quad in \quad 1 \quad cycle} \tag{12}$$

$$R_2 = \frac{PEV \quad Energy \quad Consumption \quad in \quad 1 \quad cycle}{Consumer \quad Energy \quad Demand \quad in \quad 1 \quad cycle} \tag{13}$$

Table III is the gist of this study. Dumb- and optimal charging methods are compared in detail with respect to another two terms: R_3 and R_4. The maximum PEV energy consumption in the considered time cycle is noted. Say, this occurs at hour t_c, termed as critical hour. The difference between the consumer

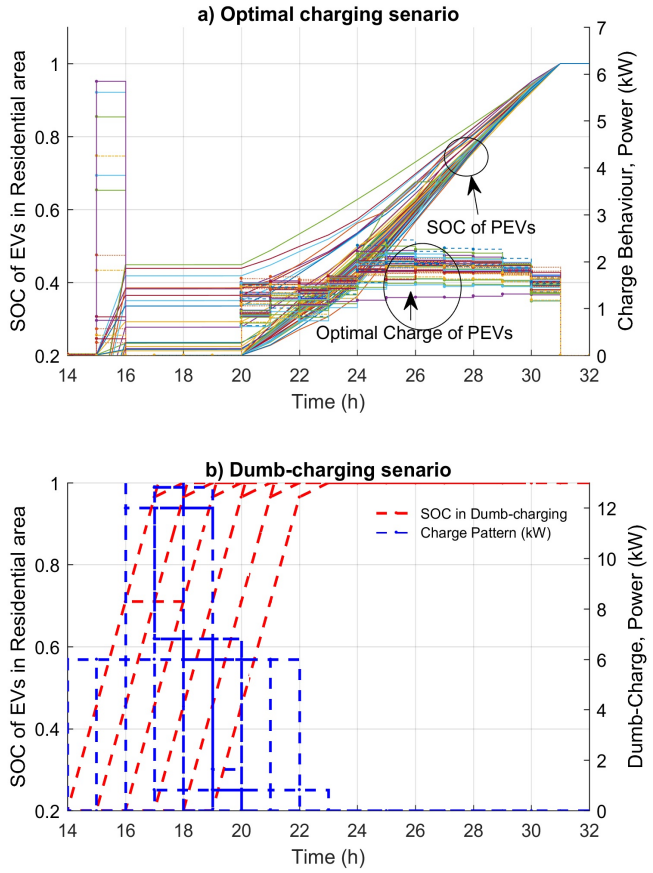

Fig. 5. 70% PEV and 100% PV penetration in the distribution grid. Charge behavior and SOC of the PEVs located at the residential area a) with the proposed algorithm b) with dumb-charging method

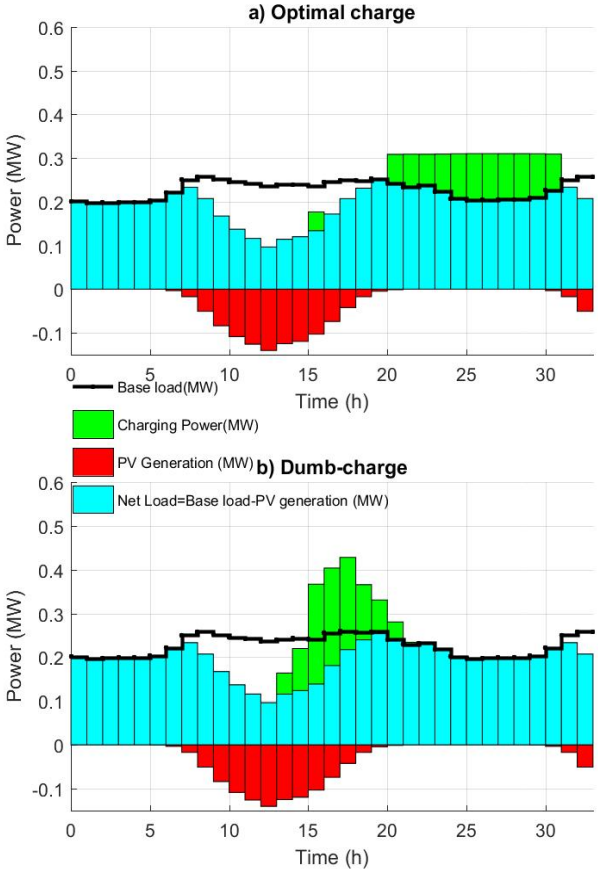

Fig. 6. Share of base load, 70% PEV load and 100% PV generation at the secondary of transformer DT1 shown in Fig. 2. a) Optimal charge behavior. Binding loading constraint on transformer DT1 makes a flat profile from hour 21 until 30. b) Dumb-charge behavior.

energy demand and PV generation in this instance t_c is noted. The term R_3 is defined as follows:

$$R_3 = \frac{Max \quad PEV \quad Energy \quad Consumption \quad at \quad t_c}{(Consumer \quad Energy \quad Demand - \quad PV \quad Generation) \quad at \quad t_c} \tag{14}$$

$$R_4 = A + B - C \quad (at \quad t_c) \tag{15}$$

Where A = Consumer Energy demand, B = PEV energy consumption and C = PV generation

R_3 is almost constant for the optimal charging scenario for different levels of PEV-PV penetration; it increases when PEV penetration is 100%.

For the optimal charging scenario, the total transformer load at hour t_c is almost 315 kW, whereas for the dumb-charging scenario it is 600 kW. Also, the total cost of power import from the main grid for the optimal charging scenario is always less than that for the dumb-charging scenario, as expected.

Fig. 6 clears the concept behind Table III. Green bars show the PEV load and red bars represent PV production. PV production during hours 15-19 could alleviate the PEV load on the system for the case of dumb-charging. Total share of

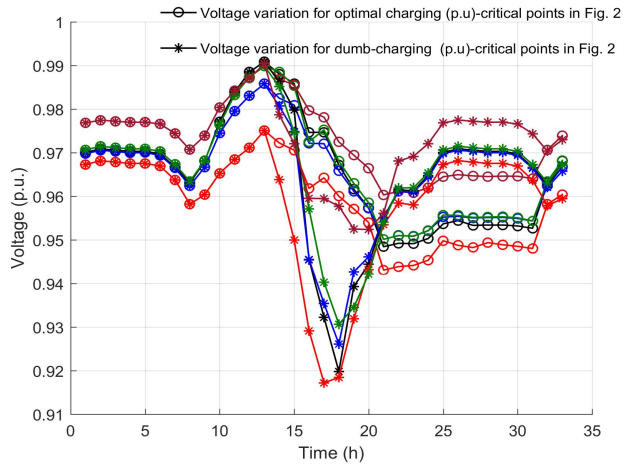

Fig. 7. Voltage variation at the critical nodes of the network with optimal charging and dumb-charging (Black: H50, Red: H23, Blue: H02, Green: H16 and Brown: H33). 70% PEV and 100% PV in the network.

TABLE II
VARIATION OF R_1 AND R_2 FOR DIFFERENT PEV-PV PENETRATION LEVELS FOR ONE-CYCLE 0800 - 0800

PEV-PV(%)	0-0	10-10	20-20	30-30	40-40	50-50	60-60	70-70	80-80	90-90	100-100
R_1	0	0.84	2.89	4.03	6.19	7.32	9.77	11.20	12.81	13.40	17.74
R_2	0	2.58	5.16	7.748	10.33	12.91	15.49	18.07	20.66	23.56	26.15

TABLE III
VARIATION OF R_3, R_3, AND MINIMISED COST OF POWER IMPORT FOR DIFFERENT PEV-PV PENETRATION LEVELS

PEV-PV(%)		0-0	0-30	0-70	0-100	30-0	30-30	30-70	30-100	70-0	70-30	70-70	70-100	100-0	100-30	100-70	100-100
Dumb-Charging method	R_3	-	-	-	-	45.12	50.57	62.67	79.29	95.3	106.7	132	167	143	160	198	251
	R_4	-	-	-	-	348	321	277	239	480	451	406	367	603	573	527	486
	Cost (€)	6969	6391	5760	4994	6990	6453	5821	5055	7121	6543	5910	5144	7191	6611	5978	5211
Optimal Charging method	R_3	-	-	-	-	53.4	53.4	53.4	53.4	54	54	54	54	Infeasible	Infeasible	78	106
	R_4	-	-	-	-	310	310	310	310	310	310	310	310			313	310
	Cost (€)	6969	6391	5760	4994	7031	6355	5664	4820	7025	6388	5697	4853			5895	5119

PEV in comparison with consumer load demand is noticeable as well.

Fig. 7 represents the voltage profile of critical nodes at the network as shown in Fig. 2 The result is for the case of 70% PEV and 100% PV in the network.

V. CONCLUSIONS

This paper presents a multi-period ACOPF including storage equations to simulate a large-scale PEV-PV penetration in a distribution grid also consisting of small wind generators and hydropower. The simulation results suggest that the proposed approach is advantageous over the traditional uncontrolled charging methodology. First, it minimises the total cost of power imported into the distribution system from the main grid. Further, it can be used to schedule charging optimally to satisfy the distribution grid constraints. The studies conducted demonstrate that flexibility can be introduced in the system through appropriate PEV integration.

REFERENCES

[1] S. Allard, P. C. See, M. Molinas, O. B. Fosso, and J. A. Foosns, "Electric vehicles charging in a smart microgrid supplied with wind energy," in *IEEE PowerTech Conference*, Jun. 2013, pp. 1–5.

[2] A. M. A. Haidar, K. M. Muttaqi, and D. Sutanto, "Technical challenges for electric power industries due to grid-integrated electric vehicles in low voltage distributions: A review," *Energy Conversion and Management*, vol. 86, pp. 689–700, Oct. 2014.

[3] M. Liu, P. McNamara, R. Shorten, and S. McLoone, "Residential electrical vehicle charging strategies: the good, the bad and the ugly," *Journal of Modern Power Systems and Clean Energy*, vol. 3, no. 2, pp. 190–202, Jun. 2015.

[4] S. Shao, M. Pipattanasomporn, and S. Rahman, "Challenges of PHEV penetration to the residential distribution network," in *IEEE Power Energy Society General Meeting*, Jul. 2009, pp. 1–8.

[5] M. Khanabadi, S. Moghadasi, and S. Kamalasadan, "Real-time optimization of distribution system considering interaction between markets," in *2013 IEEE Industry Applications Society Annual Meeting*, Oct. 2013, pp. 1–8.

[6] S. Moghadasi and S. Kamalasadan, "Real-time optimal scheduling of smart power distribution systems using integrated receding horizon control and convex conic programming," in *IEEE Industry Application Society Annual Meeting*, Oct. 2014, pp. 1–7.

[7] J. Carpentier, "Contribution to the economic dispatch problem," *Bulletin de la Socit Franaise des Electriciens*, vol. 8, pp. 431–447, 1962.

[8] M. Huneault and F. D. Galiana, "A survey of the optimal power flow literature," *IEEE Transactions on Power Systems*, vol. 6, no. 2, pp. 762–770, May 1991.

[9] J. A. Momoh, R. Adapa, and M. E. El-Hawary, "A review of selected optimal power flow literature to 1993. I. Nonlinear and quadratic programming approaches," *IEEE Transactions on Power Systems*, vol. 14, no. 1, pp. 96–104, Feb. 1999.

[10] S. Frank, I. Steponavice, and S. Rebennack, "Optimal power flow: a bibliographic survey I," *Energy Systems*, vol. 3, no. 3, pp. 221–258, 2012.

[11] F. Rahimi and A. Ipakchi, "Demand response as a market resource under the smart grid paradigm," *IEEE Transactions on Smart Grid*, vol. 1, no. 1, pp. 82–88, Jun. 2010.

[12] F. Pilo, G. Pisano, and G. G. Soma, "Optimal coordination of energy resources with a two-stage online active management," *IEEE Transactions on Industrial Electronics*, vol. 58, no. 10, pp. 4526–4537, Oct. 2011.

[13] A. Kumar and W. Gao, "Optimal distributed generation location using mixed integer non-linear programming in hybrid electricity markets," *IET Generation, Transmission and Distribution*, vol. 4, no. 2, pp. 281–298, Feb. 2010.

[14] R. Tonkoski, D. Turcotte, and T. H. M. EL-Fouly, "Impact of high PV penetration on voltage profiles in residential neighborhoods," *IEEE Transactions on Sustainable Energy*, vol. 3, no. 3, pp. 518–527, Jul. 2012.

[15] Ø. Sagosen, "Analysis of large scale integration of electric vehicles in Nord-Trøndelag," *Master Thesis, NTNU*, 2013. [Online]. Available: https://brage.bibsys.no/xmlui/handle/11250/257521